Springer

Journal of
Mechanical
Science and
Technology

Journal of Mechanical Science and Technology 23 (2009) 536~543

www.springerlink.com/content/1738-494x
DOI 10.1007/s12206-008-1013-5

Experimental measurement and numerical computation of the air side convective heat transfer coefficients in a plate fin-tube heat exchanger †

Jin Gi Paeng[1], Kyung Hwan Kim[2] and Young Hwan Yoon[3]

[1]*Department of Mechanical Engineering, Changwon National University*
[2]*Division of Facilities, Changwon National University*
[3]*Department of Mechanical Engineering, Changwon National University*

(Manuscript Received January 10, 2008; Revised October 2, 2008; Accepted October 20, 2008)

Abstract

The air-side forced convective heat transfer of a plate fin-tube heat exchanger is investigated by experimental measurement and numerical computation. The heat exchanger consists of a staggered arrangement of refrigerant pipes with a diameter of 10.2 mm and a fin pitch of 3.5 mm. In the experimental study, the forced convective heat transfer was measured at Reynolds numbers of 1082, 1397, 1486, 1591 and 1649 based on the diameter of the refrigerant piping and on the maximum velocity. The average Nusselt number for the convective heat transfer coefficient was also computed for the same Reynolds number by using the commercial software STAR-CD with the standard $k-\varepsilon$ turbulent model. It was found that the relative errors of the average Nusselt numbers between the experimental and numerical data were less than 6 percent in a Reynolds number range of 1082~1649. The errors between the experiment and other correlations from literature ranged from 7% to 32.4%. However, the literature correlation of Kim et al. is closest to the experimental data within a relative error of 7%.

Keywords: Air-side convective heat transfer; Plate fine-tube heat exchanger; Average Nusselt number

1. Introduction

Domestic manufacturers produce several types of flat plate fin tube heat exchangers. These types of heat exchangers are typically fabricated via the mechanical expansion of circular pipes to flat plate fins. It has been reported that the overall heat transfer coefficient changes by as much as 20 % depending on the manufacturer. However, the manufacturers did not supply precise technical data to designers of air conditioning systems. One reason may be that it is very expensive and time consuming for a manufacturing company to acquire this technical data.

One purpose of this study was to measure the air side heat transfer coefficient of a certain domestic flat plate fin-tube heat exchanger where the coefficient dominates the overall heat transfer coefficient. The experimental heat transfer coefficients were then compared with several correlations from literature.

The first correlation is from Kays and London [1]. It connected the rate of heat transfer with the Reynolds number based on the equivalent diameter for the passage of an air flow. In addition, the equations of Wang et al. [2], Kim et al. [3], and Gray and Webb [4] associated the Nusselt number with the Reynolds number based on the diameter of the refrigerant pipe. In all of the aforementioned equations from the literature, the thermodynamic properties of fluid were based on the film temperature.

Another purpose of this study was to predict the rate

† This paper was recommended for publication in revised form by Associate Editor Man-Yeong Ha

* Corresponding author. Tel.: +82 2 279 7501, Fax.: +82 2 275 0101
E-mail address: gjpaeng@changwon.ac.kr

of heat transfer by numerical computation using the commercial software STAR-CD. For this study, Chung et al. [5] and Ko et al. [6] computed the two-dimensional turbulent flow between fins. Additionally, Yun et al. [7] simulated a three-dimensional laminar flow in the computational domain. However, many designers currently use commercial software to simulate three-dimensional turbulent flows in any arbitrary geometry. Therefore, it is also necessary to verify the accuracy of the commercial software used in as many applications as possible.

In the present study, the air-side forced convection heat transfer was measured and computed at = 1082, 1397, 1486, 1591, and 1649 from operational conditions for a general home air-conditioner. The corresponding Nusselt numbers were evaluated with equations from Kays and London [1], Wang et al. [2], Kim et al. [3], and Gray and Webb [4]. Finally, comparisons were made between the experimental data and the data from the literature, as well as between the experimental data and numerical data.

2. Heat transfer correlations

2.1 Description of a Flat Plate Heat Exchanger

The configuration of the fin-and-tube heat exchanger in this study is shown in Fig. 1 Refrigerant pipes of Φ10.2 mm are staggered and the pitch between the fins is 3.5 mm. Schematic drawings of the fins and tubes are given in Fig. 2, and Table 1 shows the related dimensions.

2.2 Derivation of the air-side nusselt number

The air-side Nusselt number can be obtained though the following mathematical relationship:

$$\dot{Q} = \eta_t h A_t \Delta T = \eta_t h A_t (T_w - T_f) \tag{1}$$

In this equation:

η_t : total fin efficiency
h : air-side average heat transfer coefficient
A_t : total exposed surface area
T_w : surface temperature of refrigerant pipe
T_f : bulk temperature of air

The total fin efficiency, η_t , is defined by Eq. (2)

Table 1. Geometric dimension of the fins and tubes.

[unit : mm]

Type	D	P_t	P_l	P_f	S	t	N
Plate	10.2	25	22	3.53	3.2	0.33	3

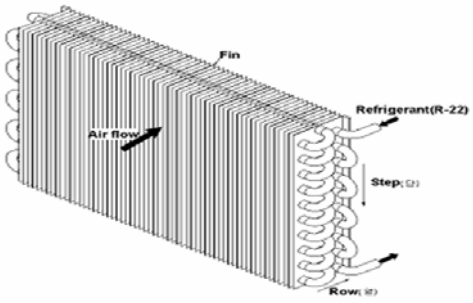

Fig. 1. Flat plate fin-tube heat exchanger.

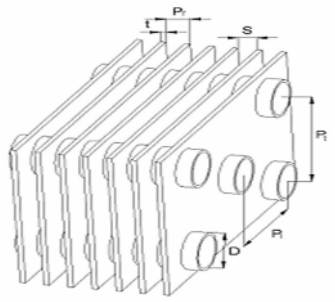

Fig. 2. Schematic of assembled fins and tubes.

$$\eta_t = 1 - \frac{A_f}{A_t}(1 - \eta_f) \tag{2}$$

where η_f is fin efficiency from Schmidt's equation [8].

The bulk temperature of air, T_f, is simply assumed as the mean temperature between the inlet temperature T_{in} and the outlet temperature T_{out} of the heat exchanger. [9, 10]

$$T_f = \frac{T_{in} + T_{out}}{2} \tag{3}$$

The average heat transfer coefficient is derived from Eq. (1).

$$h = \frac{\dot{Q}}{\eta_t A_t (T_w - T_f)} \tag{4}$$

Additionally, the average Nusselt number is expressed as Eq. (5) with its definition for the diameter of the pipe, D, and the thermal conductivity.

$$Nu_D = \frac{\dot{Q}}{\eta_t A_t (T_w - T_f)} \cdot \left(\frac{D}{k_f} \right) \tag{5}$$

2.3 Correlations of the nusselt number from the literature

Several correlations of the Nusselt number for an air-side convective heat transfer from the literature are listed below to compare them with numerical and experimental results.

2.3.1 Kays and London equation

The correlation equation for a Nusselt number by Kays and London is given as Eq. (6).

$$Nu_{D_h} = \frac{0.011 \cdot \mathrm{Re}_{D_h}^{-0.418} G_{\max} C_p}{\mathrm{Pr}^{2/3}} \left(\frac{D_h}{k_f} \right) \tag{6}$$

The hydraulic diameter D_h in Eq. (6) above is defined as Eq. (7) based on the minimum free area for an air flow. The Reynolds number is also defined with the maximum mass flow rate ($G_{\max} = \rho V_{\max}$) and the hydraulic diameter by Eq. (8)

$$D_h = \frac{4_{\min} L}{A_t} \tag{7}$$

$$\mathrm{Re}_{D_h} = \frac{G_{\max} 4\gamma_h}{\mu} = \frac{G_{\max} D_h}{\mu} \tag{8}$$

2.3.2 Equation by wang et al.

Wang et al. suggested Eq. (9) through experimental data between 450 < Re_D < 7500 when the number of rows in a heat exchanger, N, is greater than 2.

$$Nu = \frac{0.086 \mathrm{Re}_D^{P_3} N^{P_4} \left(\frac{P_f}{D} \right)^{P_5} \left(\frac{P_f}{D_h} \right)^{P_6} \left(\frac{P_f}{P_t} \right)^{-0.93} \frac{G_{\max} C_P}{\mathrm{Pr}^{2/3}} D}{k_f} \tag{9}$$

$$P_3 = -0.361 - \frac{0.042N}{\ln(\mathrm{Re}_D)} + 0.158 \ln \left[N \left(\frac{P_f}{D} \right)^{0.41} \right]$$

$$P_4 = -1.224 - \frac{0.076 \left(\frac{P_l}{D_h} \right)^{1.42}}{\ln(\mathrm{Re}_D)}$$

$$P_5 = -0.083 + \frac{0.076N}{\ln(\mathrm{Re}_D)}$$

$$P_6 = -5.735 + 1.21 \ln \left(\frac{\mathrm{Re}_D}{N} \right)$$

2.3.3 Equation by Kim et al.

Kim et al. also suggested an equation, Eq. (10), for the average Nusselt number when N>3.

$$Nu_S = \frac{0.163 \mathrm{Re}_D^{-0.369} \left(\frac{P_t}{P_l} \right)^{0.106} \left(\frac{S}{D} \right)^{0.0138} \left(\frac{P_t}{D} \right)^{0.13} \frac{G_{\max} C_P}{\mathrm{Pr}^{2/3}} D}{k_f} \tag{10}$$

2.3.4 Gray and Webb equation

Lastly, Gray and Webb suggested Eq. (11) through experimentation.

$$Nu = \frac{0.991 Nu_4 \left[2.24 \mathrm{Re}_D^{-0.092} \left(\frac{N}{4} \right)^{-0.031} \right]^{0.607(4-N)} \frac{G_{\max} C_P}{\mathrm{Pr}^{2/3}} D}{k_f} \tag{11}$$

3. Experiments of heat exchanger

3.1 Experimental apparatus

The experimental apparatus consists of an evaporator, a compressor, a condenser and an expansion

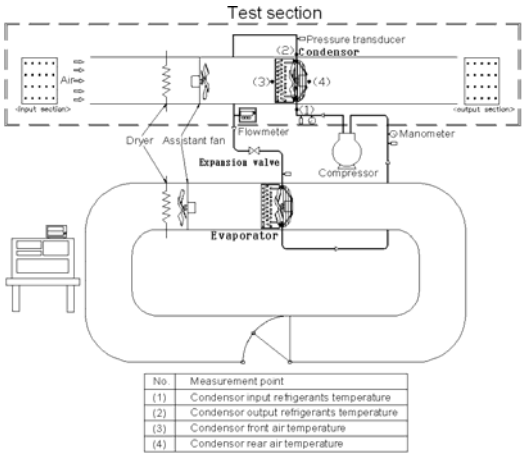

Fig. 3. Schematic diagram of the experimental apparatus for a heat exchanger.

Table 2. Specifications of the experimental apparatus.

Equipment		Specification
Compressor		0.5 HP
Duct	Condensor	360×270×1500 mm
Refigerant		R-22
Refigerant flow meter		Electronic type
Pressure transducer		0~35 bar

valve through which the refrigerant R-22 circulates, as shown in Fig. 3. The condenser is cooled by a straight air duct with the dimensions of 360x270x 1500 mm. An electric heater powered at 9 kW(1.5 kWx6) is installed 150 mm from the inlet, and the speed of a fan installed 450 mm from the inlet can vary from 0 to 1700 rpm. The number of measurement points for the air velocity and temperature at both the inlet and the outlet is 20. The points are evenly distributed at each cross-section of the duct. Refrigerant temperatures at inlet and outlet of the condenser are measured with T-type thermocouples. The general specifications of the experimental apparatus are given in Table 2.

3.2 Experimental method

Testing of the experimental apparatus started after the steady state which required approximately 40-60 minutes and during which the variations at the inlet and outlet pipes of the condenser were within ± 0.1℃. The temperature and velocity at each aforementioned point were determined in three separate measurements at 30 seconds intervals by using a hot-wire anemometer with an accuracy of 2% in terms of the velocity and at a temperature of ± 0.5℃ (model: Testo 650). The mean air temperature before the heat exchanger (condenser) was maintained at 31℃ by controlling the power of an electric heater. The air velocity in the duct was changed by controlling the speed of the fan motor. The velocity increased from 1.13 m/s to 1.61 m/s in five steps with Reynolds numbers that ranged from 1082 to 1649, as given in Table 3.

3.3 Experimental results

The heat transfer rate of air through the heat exchanger can be expressed by Eq. (12).

Table 3. Heat transfer rate of air from measured data.

Re_D	Temperature		Velocity [m/s]	Heat transfer rate Q_w [W]
	In	Out		
1082	31	53.8	1.09	1094
1397	31	42	1.37	1357
1486	31	41.5	1.45	1473
1591	31	41.8	1.56	1543
1649	31	41.7	1.61	1689

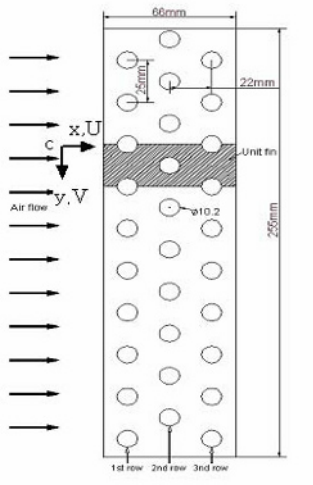

Fig. 4. Dimensions for the modeling of the fin.

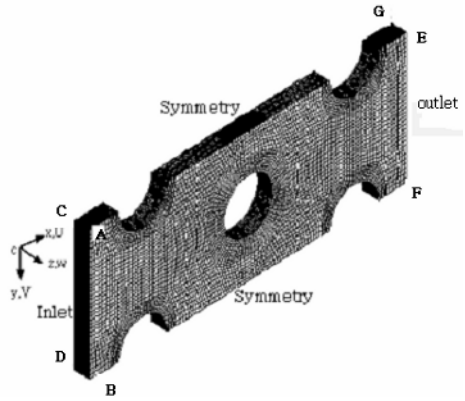

Fig. 5. Configuration of cells in the 3-D computational control volume.

$$\dot{Q} = \rho U_{mean} A C_p \Delta T = \dot{m}_{air} C_P \left(T_{out} - T_{in}\right) \qquad (12)$$

Here, $\dot{m}_{air}$ denotes the mass flow rate of air, and T_{in} and T_{out} are the air temperatures before and after the heat exchanger. The rate of heat transfer in Eq. (12) was also computed with the measured data at various Reynolds numbers, as shown in Table 3.

4. Numerical computation

4.1 Modeling of the mesh

The computational grids are modeled in a control volume consisting of a fin interval of 3.2 mm and the slashed surface area of the fin shown in Fig. 4.

Air enters at the ABDC cross-section and comes out at the EFHG section. As shown in the figure, one circular cylinder in the middle of the domain and four half circular cylinders at four corners of the domain represent the refrigerant pipes. The inlet (3.2 x 25 mm^2) is divided into 40 x 34 cells so that the total number of cells and the vertex are 341,184 and 358,925 including 39,936 solid cells corresponding to the half thickness of a fin. In addition, the cells become smaller as they approach the wall. Mesh information regarding the number of grids and the lengths is given in Table 4.

4.2 Governing equations for the numerical computation

Eq. (13), Eq. (14) and Eq. (15) are the continuity equation, the momentum equation, and the energy equation which together govern the fluid flow in the control volume.

$$\frac{\partial U_i}{\partial X_i} = 0 \tag{13}$$

$$U_j \frac{\partial U_i}{\partial x_j} = -\frac{1}{\rho}\frac{\partial p}{\partial x_i} + \frac{\partial}{\partial x_j}\left(\nu \frac{\partial U_i}{\partial x_j} - \overline{u_i' u_j'}\right) \tag{14}$$

$$U_j \frac{\partial T}{\partial x_j} = \frac{\partial}{\partial x_j}\left(\alpha \frac{\partial T}{\partial x_j} - \overline{T u_j'}\right) \tag{15}$$

The turbulent stress term $-\overline{u_i' u_j'}$ of Eq. (14) is defined as Eq. (16)

$$-\overline{u_i' u_j'} = \frac{\mu_t}{\rho}\left(\frac{\partial u_i}{\partial x_j} + \frac{\partial u_j}{\partial x_j}\right) - \frac{2}{3}\delta_{ij} k \tag{16}$$

Table 4. Mesh information in the control volume.

Region	Grid	Distance [mm]	Region	Grid	Distance [mm]
a-b	34	25	a-e	110	66
a-c	40	3.2	e-g	40	3.2
c-d	34	25	e-h	34	25

where δ_{ij} is Kronecker's δ and μ_t is the turbulent viscosity defined by Eq. (17) with the turbulent kinetic energy k and the turbulent dissipation energy ε. The standard $k-\varepsilon$ model for a high Reynolds number is used for the turbulent flow [11].

$$\mu_t = C_\mu \rho \frac{k^2}{\varepsilon} \tag{17}$$

4.2 Boundary conditions

As the fluid in the control volume is three-dimensional, steady state, and because it has a turbulent flow, the computation requires six variables. These are three velocity components (U, V, W) according to the Cartesian coordinates (x, y, z), k and ε for the turbulent flow, and T for the temperature. Therefore, elliptic boundary conditions for the six variables must be determined.

4.3.1 Inlet boundary condition

The principal velocity component U_{in} was measured by using a velocity meter for the inlet boundary condition, and the perpendicular velocity components of V_{in} and W_{in} were assumed to be zero as expressed by Eq. (18).

$$U_{in} = U_{mean},\ V_{in} = 0,\ W_{in} = 0 \tag{18}$$

The turbulent kinetic energy, k, can be expressed by Eq. (19) with the mean velocity U_{mean} and turbulent intensity I at the inlet of the numerical domain.

$$k = 1.5 \times \left(U_{mean} \times I\right)^2 \tag{19}$$

It was found that I = 10% is most reasonable as the inlet condition through a comparison between the numerical and experimental heat transfers. Eq. (20) is an expression of the turbulent dissipation energy where the turbulent coefficient C_μ is 0.09 and the turbulent mixing length ℓ is 0.27 mm with a 10% interval between the fins.

$$\varepsilon = C_\mu^{0.75} \times \frac{k^{1.5}}{l} \tag{20}$$

The air temperature was also measured for the inlet condition, as expressed by Eq. (21).

$$T = T_{in} \tag{21}$$

4.3.2 Exit boundary condition

A Neumann condition was applied at the exit of the computational domain, as expressed by Eq. (22).

$$\frac{\partial U_i}{\partial x} = \frac{\partial k}{\partial x} = \frac{\partial \varepsilon}{\partial x} = \frac{\partial T}{\partial x} = 0 \tag{22}$$

In addition, the pressure condition(p=0) was also applied at the exit for comparison of the exit boundary condition. The pressure condition, however, showed a much greater error of 48% compared with the experimental data in spite of the fact that the fully developed condition showed only 6 % of relative error with the experimental data.

4.3.3 Wall boundary condition

The non-slip condition for the fluid flow was used at walls, as given in Eq. (23).

$$U_{wall} = V_{wall} = W_{wall} = 0 \tag{23}$$

Furthermore, k and ε near the wall were obtained from the wall function with a non-slip condition.

For the temperature boundary condition, the temperature gradient was assumed to be zero at the middle of the fin thickness. Additionally, the wall temperature of the refrigerant pipes was determined through the saturation temperature of the refrigerant in the condenser.

4.3 Computational results

The Reynolds numbers in the computation were 1082, 1397, 1486, 1591, and 1649 based on the mean air velocity and diameter of the refrigerant pipes running perpendicular to the fins.

Fig. 6 presents x-direction velocity contours at the middle plane between the fins when the Reynolds number is 1486. In the contour, the velocities appear symmetric and become fast closer to four half circles and a middle circle.

Fig. 7 shows contours of the fluid temperature under the same condition. This figure shows that the air temperature becomes higher behind the refrigerant pipes. If the rate of heat transfer is integrated through all surfaces, the average Nusselt number can be obtained via Eq. (4).

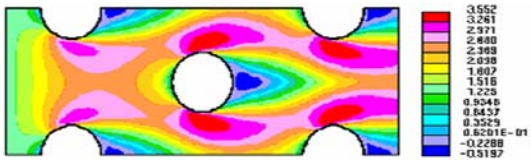

Fig. 6 Contours of the U-component velocity (Re_D = 1486) [unit: m/s]

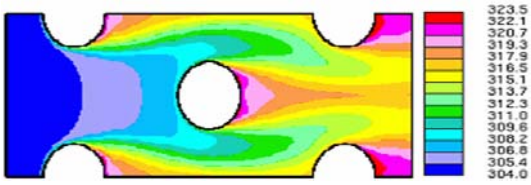

Fig. 7 Contours of the air temperature (Re_D = 1486) [unit: K]

5. Comparison between experiments and computation

The average Nusselt numbers for the design equation from the numerical computations and experiments can be expressed as $Nu_D = C_1 \cdot \mathrm{Re}_D{}^m \cdot \mathrm{Pr}_f^{1/3}$ by a dimensional analysis. Here, Pr_f, the Prandtl number of the fluid, is assumed to be 0.69 up to a temperature of 600 K. Thus, the equation has the form of $Nu_D = C_1 \cdot \mathrm{Re}_D^m$. Eq. (24) is the correlation equation from the experimental data by the least square method for log coordinates from Reynolds numbers of 1082 to 1649.

$$Nu_D = 0.049 \cdot \mathrm{Re}_D^{0.784} \cdot \mathrm{Pr}_f^{1/3} = 0.044 \cdot \mathrm{Re}_D^{0.784} \tag{24}$$

Eq. (25) is derived from numerical data in the same manner as Eq. (24).

$$Nu_D = 0.11 \cdot \mathrm{Re}_D^{0.671} \cdot \mathrm{Pr}_f^{1/3} = 0.097 \cdot \mathrm{Re}_D^{0.671} \tag{25}$$

Fig. 8 compares Eq. (24) from the experiments and Eq. (25) from the numerical computation. This figure shows that the relative errors are from 3.5 % to 5.7 % depending on the Reynolds number.

Fig. 9 shows comparisons among the correlation equation from the experiments and the equations from the literature. Compared here are Eq. (8) of Kays and London [1], Eq. (9) of Wang et al. [2], Eq. (10) of Gray and Webb [3], and Eq. (11) of Kim et al. [4] with the same range of Reynolds numbers. In this figure, the ranges of relative errors between the experimental equation and each equation from the

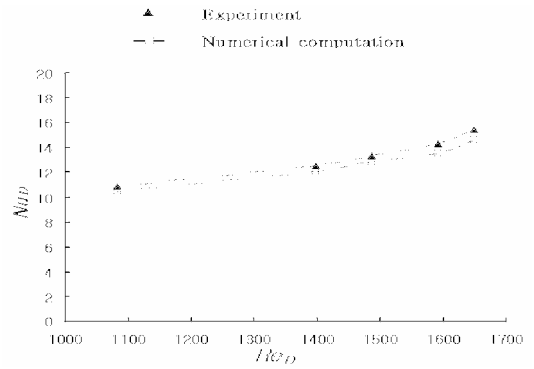

Fig. 8 Comparison of the average Nusselt form experiments and numerical computations

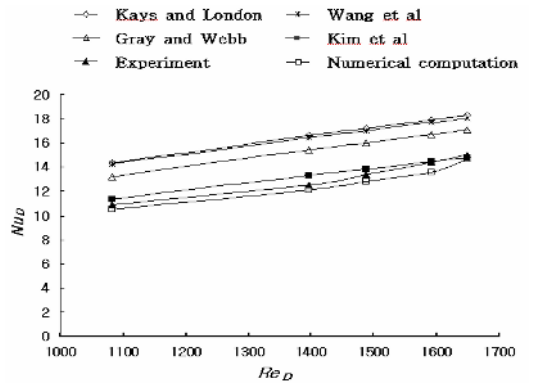

Fig. 9 Comparison of average Nusselt number, from experiments, numerical computations and the literature

literature are 17.9-32.4 % for Kays and London [1], 16.5-31.2 % for Wang et al. [2], 0.4-6.0 % for Kim et al. [4], and 10.1-23.0 % for Gray and Webb [3].

6. Conclusions

Experiments were conducted on the rate of heat transfer from staggered refrigerant pipes to flat plate fins by the air flow from Reynolds numbers that ranged from 1082 to 1649. The correlation equation from the experiments was compared with the equation from a numerical computation as well as several equations from the literature. The findings are summarized below.

(1) The Nusselt number equations from the experiments and the numerical computation are $Nu_D = 0.044\,\mathrm{Re}_D^{0.784}$ and $Nu_D = 0.097\,\mathrm{Re}_D^{0.671}$, respectively. The relative errors between these equations are 6 %; hence, the numerical computation simulates the experimental data fairly well when the Prandtl number of the air is 0.69.

(2) Numerical results with the Neumann condition at the exit of the computational domain were much closer to the experimental results compared to those with pressure condition at the exit.

(3) The correlation equation of Kim et al. from literature shows that the relative errors to the experimental data are within 7 %; thus, this equation is closest to the equation from the experiments. However, the relative errors of Gray and Webb and from Kays and London show errors in ranges of 10.1-23.0 % and 17.9-32.4 %, respectively. The equation of Wang et al. presents the largest error range of 16.5-31.4 % among all equations from the literature included here.

Acknowledgment

This work was financially supported by the Ministry of Education and Human Resources Development (MOE), the Ministry of Commerce, Industry and Energy (MOCIE) and the Ministry of Labor (MOLAB) through the fostering project of the Industrial-Academic Cooperation Centered University

References

[1] W. M. Kays and A. L. London, Compact heat exchangers, second edition, McGraw Hill. (1955) 7-224.

[2] C. C. Wang, K. Y. Chi and C. J. Chang, Heat transfer and friction characteristics of plain fin-and-tube heat exchangers. *Part Ⅱ: Int. J. Heat Mass Trans*. 43 (2000) 2693-2700.

[3] N. H. Kim, B. Youn and R. L. Webb, Air-side heat transfer and friction correlation for plain fin and tube heat exchangers with staggered tube arrangements, *J. Heat Transfer*. 121 (1999) 662-667.

[4] D. L. Gray and R. L. Webb, Heat transfer and friction correlations for plate fin and tube heat exchangers having plain fins, Proc. of the 9th International Heat Transfer Conference, *Taylor & Francis*, London, San Francisco. (1986) 2475-2750.

[5] Y. K. Chung and K. S. Lee, Heat and flow analysis of a parallel flow heat exchanger, *Society of Air-Conditioning and Refrigerating Engineers of Korea.* (2001) 424-430.

[6] S. H. Ko, H. G. Park, B. K. Park and J. C. Kim, Numerical analysis on the condensation heat transfer and pressure drop characteristics of the horizontal tubes of modular shell and tube-bundle heat exchanger. *The Korean Society of Mechanical Engineers*. (2001) 191-198.

[7] J. W. Yun, J. Y. Yun and M. H. Kim, Numerical study on the characteristics of flow and heat transfer in fined tube heat exchanger, *Society of Air-Conditioning and Refrigerating Engineers of Korea*. (1995) 74-79.

[8] T. E. Schmidt, Heat transfer calculation for extended surfaces, *Journal of ASRE, Refrigerating Engineering*, 4 (1949) 315-357.

[9] H. C. Kang, M. H. Kim, J. Y. Yun and H. Y. Kim, A Large scale model test to investigate the thermo-hydraulic characteristics in the air side of exchanger for air-conditioner, *Society of Air-Conditioning and Refrigerating Engineers of Korea*. (1995) 42-47.

[10] H. C. Kang and M. H. Kim, Thermohydraulic characteristics of multi-row, plane finned-tube heat exchanger for air-conditioner, *Society of Air-Conditioning and Refrigerating Engineers of Korea*. (1996) 315-321.

[11] Star-CD, Methodology V3.15A, (1999) 2.5-2.6.

Jin-Gi Paeng recieved a bachelor´s degree in Aero Mechanical Engineering from Gyeong-sang National University in 2000. He then went on to recieve his M.S. degrees from Changwon National University in 2004. Currently, he completed the doc-tor´s course and a doctoral dissertation in 2007 and 2008, respectively. He will take a doctorate in 2008.